International Journal of Academic Engineering Research (IJAER)
ISSN: 2643-9085
Vol. 5 Issue 3, March - 2021, Pages: 51-58

Atomic Distributions Observed In Group Iv-Iv Binary Tetrahedron Alloys: A Revised Analysis Of Sige And Gesn Compounds

Jurabek Abdiyev[1],Sadulla Saydullayev[1], Elyor G'aybulloyev[2], Sherzod Yarashev[2*], Bekzod Erkinov[2]

[1]Physical-technical Institute of NPO "Physics – Sun" of Uzbekistan Academy of Sciences Uzbekistan, Tashkent, Chingiz Aitmatov street 2B.

[2]Tashkent University of Information Technologies named after Muhammad al-Khwarizmi, Uzbekistan, Tashkent, Amir Temur street 108.

Corresponding author: sherzodyarashev1997@gmail.com (Sh. Yarashev)

Abstract: *This manuscript is an attempt to extend the Strained Tetrahedron Model to the interpretation of the EXAFS spectra of Group-IV-IV binary tetrahedron ordered B3 zinc blende alloys. The analysis clearly points out the difference of these systems respect to other binary alloys. To illustrate and describe the application of the Strained Tetrahedron Model a revised characterization of $Ge_{1-x}Si_x$ and $Ge_{1-x}Sn_x$ alloys is presented and discussed.*

Keywords: Group IV-IV binary tetrahedron ordered alloys, Site occupation preference, GeSn, GeSi

1. INTRODUCTION.

Carbon as other Group-IV elements: Si, Ge, Sn and Pb, can crystallize in the cubic allotropic variety, characterized by the tetrahedron ordered diamond (B4) crystal structure. Their binary alloys within the Group-IV elements also can crystallize as tetrahedron ordered zinc blende (B3) crystal structures. Tetrahedron configured crystal structures have one atom at the center and four at the apexes of the elemental tetrahedron. In GroupeIIIeV, GroupeIIeVI and Group-I-VII alloys, an ion of one group occupies the central configuration position, while the four peripheral positions are taken by ions of the other group, with rather rare anti-site exceptions. In Group-IV-IV alloys all atoms are fundamentally ambi-site free to take either of the two positions. Thus canonically one has to develop, for AB binary Group-IV-IV alloys a model useful for their analysis.

In tetrahedron configured B3 AB binary Group-IV-IV alloys, we have ten configurations, of which four are regular tetrahedra known in the literature, while six are strained tetrahedra to be determined (cf. Appendix). In the 1980's the local structure of crystalline and amorphous SiGe binary alloys were intensively studied by EXAFS spectroscopy Refs. [1e3] using the theoretical models available at the time Refs. [1e9]. In 1999 Aubry et al. Ref. [10] analyzed the EXAFS spectra for c-$Ge_{1-x}Si_x$ alloys grown by molecular beam epitaxy (MBE), measuring both the Ge K-edge x-ray absorption spectra (XAS) at the Cornell High Energy Synchrotron Source (CHESS) and the Si K-edge XAS at the Canadian Synchrotron Facility at the Synchrotron Radiation Center (SRC) line in Stoughton. High quality spectra at both Si and Ge K-edges allowed to identify accurate interatomic distances vs. the relative content x. Data pointed out a significant disagreement with the theoretical model, still unresolved. This open scenario motivated the present analysis.

For Groups III-V, II-VI and I-VII ternary compounds a successful attempt to resolve the disagreement with experimental observations was obtained introducing the Strained Tetrahedron Model (STM) Refs. [11,12]. The model is presently being extended to Group IV-IV tetrahedron structured binary alloys.

In Ref. [11] we developed the STM to interpret EXAFS spectra of B3 and B4 ternary alloys; to recover from observed EXAFS spectra the three SOP W-coefficients, one needs 3 N_i observed values, while to obtain the R_i values, besides the3*2 R_i observed values, one needs the corresponding lattice parameter a [Å] (Table A1). SOP W-coefficients can be determined when N_i values are not observed provided 3*2þ3 R_i values are observed. In Ref. [12] was also introduced a Statistical model to interpret FIR spectra of B3 and B4 ternary alloys; the Kramer-Kronig treatment of experimental FIR spectra yields abscissa in absolute units, but ordinates in relative units, requiring to be normalized knowledge of both dielectric constants, static ε_0 and dynamic ε_∞ (Table A1). In Ref. [13] we extended the interpretation to Heusler $L1_2$ ternary alloys and in Refs. [14] to B3 structured pseudo-quaternary $A_{1-x}B_xY_yZ_{1-y}$ systems. Later in Ref. [15] EXAFS and FIR observations of B4 crystal were compared and it was applied to the hydrogenation of a CdTe sample Ref. [16] by FIR. In Ref. [17] Laves phase C15 ternaries were treated, in Ref. [18] a B3 truly-quaternary was analyzed while Ref. [19] is a review of the Site Occupation Preference (SOP) coefficients-W and attenuation coefficients-C investigated alloys.

These initial studies concerned Group II-VI Refs. [11,12,14e16,20e26] and III-V Refs. [11,14,18,20,22,24e31] and later Group I-VII alloys such as (KRb)Br and Rb(BrI). We now present and discuss the interpretation of EXAFS spectra of Group IV-IV tetrahedron structured binary alloys. To describe the more complex rhombohedron with its dimer chain structures requires additional parameters and a larger number of experimental observations Ref. [31]. Within these limitations the STM model is here applied to analyze the available data of two tetrahedron-structured Group IV-IV binary alloys $Ge_{1-x}Si_x$ Ref. [10] and $Ge_{1-x}Sn_x$ Ref.

[32]. The SOP coefficients W_{kj} and the corresponding attenuation factors C_{kj} of each random Bernoulli Eigen-function of the six canonical binary distorted tetrahedron configurations [(4 j)A jBTk,j]k¼A,B;j¼1,3 have been obtained using the procedure and the equations previously developed Ref. [12]. Here we use the notations relative to NN (Nearest Neighbor) and to NNN (Next Nearest Neighbor) coordi-nation numbers N_1 and N_2, [Ni.kj]i¼1,2;k¼A,B;j¼A,B; while the bond distances R_1 and R_2 are [Ri.kj]i¼1,2;k¼A,B;j¼A,B, where "i" relates to NN or NNN components, "k" to the atom at the tetrahedron center A or B, and "j" to the observed atom of the configuration around A or B.

2. The $Ge_{1-x}Si_x$ analysis

Aubry et al. Ref. [10] collected $Ge_{1-x}Si_x$ data (Table 1) on both Si and Ge K-edges. To characterize the respective configurations by the SOP-coefficients W_{kj}'s, one needs at least three N_1 values, while to determine the R_1 values six extra values are required. Our analysis was performed determining, either restrictively the SOP-coefficients, and when possible the R_1's. Indeed for both relaxed and strained samples the coverage of the x_{Si}-range is not sufficient limiting the interpretation of the SOP results.

Table 1

Looking at Fig. 6 in Refs. [10] that reports data from both Si and Ge K-edges for both relaxed thin layered with the undisturbed internal structure, and strained samples with internal stresses induced during the layer growth, we underline that within the concentration x_{Si}2[0,1] range, the coverage of the two K-edges is not uniform. For the relaxed samples for both Si and Ge K-edges data are sufficient within the x_{Si}2[0.29e0.78] range. For the strained samples Si K-edge spectra are sufficient for SOP calculations, while the four observations at the Ge K-edge allow getting the SOP-coefficients, but not the six R_1 values. Moreover, the two $N_{1.GeGe}$ are not sufficient to determine the three SOP parameters. To characterize the respective configurations by the SOP-coefficients W_{kj}'s, one needs at least three N_1 values, while to determine the R_1 values six additional values are required. The analysis has been done accordingly, determining, either restrictively the SOP-coefficients, and where possible the information on the R_1's, function of the x_{Si}-range coverage of the samples.

Fulfilling the conditions for SOP calculations (number of data number of the relative parameters) Aubrey's data are analyzed in three successive ways for the SOP analysis of available Si and Ge centered tetrahedron populations (Table 1):

1. Data in Table 1. We derive the $[W_{kj}]_{k¼A,B;\ j¼1,3}$ and $[C_{kj}]_{k¼A,B;\ j¼1,3}$ values and R_1 values of the tetrahedron configurations for both Si- and Ge- centered tetrahedra (Table 2 and Fig. 1). The obser-vations at the Si K-edge are used for the analysis of the Si-centered tetrahedra, while those at the Ge K-edge determine Ge-centered tetrahedra; the observed distribution within Si-centered configurations $^{Ge1Si}T_{Si,1}$, $^{Ge2Si}T_{Si,2}$, $^{Ge3Si}T_{Si,3}$, are respec-tively $C_{Si,1}$ ¼ 0.52, $C_{Si,2}$ ¼ 0.75, $C_{Si,3}$ ¼ 0.86, with a mean value of 0.71, while $C_{Ge,1}$ ¼ 0, $C_{Ge,2}$ ¼ 0.85, $C_{Ge,3}$ ¼ 0.81, with a mean value of 0.55. (Table 2 and Fig. 1). Actually, the mean-C_{kj}2[0,1] value is an index of how the observed distribution compare to the random Bernoulli distribution (mean ¼ 1) and to the fully or-dered distribution (mean ¼ 0) with no distorted configurations.
2. Relaxed data x_{Si}2[0.29, 0.78]. The analysis yields: $C_{Si,1}$ ¼ 0.48, $C_{Si,2}$ ¼ 0.88, $C_{Si,3}$ ¼ 0.98, with a mean value of 0.78, while $C_{Ge,1}$ ¼ 0, $C_{Ge,2}$ ¼ 0.85, $C_{Ge,3}$ ¼ 0.81, with a mean value of 0.55.
3. Strained data: all three Si-centered tetrahedra are formed, with $C_{Si,1}$ ¼ 0.62, $C_{Si,2}$ ¼ 0.52, $C_{Si,3}$ ¼ 0.54, with a mean value of 0.56. No data are reported for Ge-centered tetrahedra. N_1, N_2 and R_1, R_2 values Ref. [10] as obtained by the fit of the FT of the 1st shell EXAFS signal of $Ge_{1-x}Si_x$ alloys. Ge K-edge data are shown in italic-bold. (The parameter $N_{1.GeGe}$ ¼ 3.4 @ x ¼ 0.992 has not been considered because the value reported in Ref. [10] is physically inconsistent).

Aubry	Substrate	State	SiSi				SiGe						GeGe			
x			$R_{1.SiSi}$	.þ\-	$N_{1.SiSi}$	.þ\-	$R_{1.SiGe}$	.þ\-	$N_{1.GeGe}$	.þ\-	$N_{1.SiSi}$	.þ\-	$R_{1.GeGe}$	.þ\-	$N_{1.GeGe}$	.þ\-
0													2.45	0	4	0
0.05	Ge	Strained					2.408	0.008	3.5	0.4						
0.09	Ge	Mostly relaxed					2.398	0.015	3.7	0.8						
0.12	Ge	Strained					2.4	0.009	3.9	0.5						
0.2	Ge	Strained					2.407	0.014	3.2	0.8						
0.22	Ge	Strained					2.407	0.02	3.1	0.9						
0.29	Si	Relaxed	2.367	0.055	1.2	0.5	2.415	0.007	3.5	0.7	1.13	0.07	2.438	0.002	3.56	0.07
0.38	Ge	Relaxed	2.354	0.032	1.2	0.3	2.397	0.01	2.2	0.4						
0.42	Si	Relaxed	2.351	0.034	1.9	0.5	2.388	0.005	2.7	0.7	1.64	0.07	2.439	0.003	2.4	0.09
0.56	Si	Relaxed	2.354	0.017	2.2	0.4	2.395	0.007	1.7	0.4	2.16	0.25	2.432	0.009	2.22	
0.61	Si	Relaxed	2.355	0.013	2.4	0.2	2.388	0.005	1.7	0.3	2.35	0.07	2.435	0.004	1.52	0.07

0.78	Si	Relaxed	2.369	0.01	3.3	0.2	2.389	0.005	1.3	0.3	3.47	0.13	2.495	0.01	1.24
0.91	Si	Strained	2.35	0.009	3.2	0.2	2.388	0.003	0.6	0.2	3.55	0.14			
0.992	Si	Strained											2.396	0.008	3.4	0.3
1			2.352	0	4	0									

3

Table 2
W_{kj}, C_{kj} and R_1 values of the ambi-site tetrahedron configurations T_{Si} and T_{Ge} of $Ge_{1-x}Si_x$; Ge-centered data are in italic-thick.

K	0	1	2	3	4		S(Ck)/3 Ref. [33]
Configurations	$^{4Ge}T_{Si0}$	$^{3Ge1Si}T_{Si1}$	$^{2Ge2Si}T_{Si2}$	$^{1Ge3Si}T_{Si3}$	$^{4Si}T_{Si4}$		
	4GeTGe0	3Ge1SiTGe1	2Ge2SiTGe2	1Ge3SiTGe3	4SiTGe4		
All Table 1 data							
^{W}kj	SiSiGeGe	0.52	1.25	0.86			
		0	1.15	0.81			
^{C}kj	SiSiGeGe	0.52	0.75	0.86		0.71	
		0	0.85	0.81		0.55	
R_1	$^{R}1.SiSi$ 2.45	2.66	2.18	2.43			
	$^{R}1.SiGe$	2.32	2.36	2.38	2.352		
	$R_{1.GeSi}$[a]	Non-available[a]					
	2.45		2.32[a]	2.36[a]			
	$^{R}1.GeGe$		2.48	2.39	2.352		
Only Relaxed							
^{W}kj	SiSiGeGe	0.48	1.12	0.98			
		0	1.15	0.81			
^{C}kj	SiSiGeGe	0.48	0.88	0.98		0.78	
		0	0.85	0.81		0.38	
R_1	$^{R}1.SiSi$ 2.45	2.68	2.21	2.42			
	$^{R}1.SiGe$	2.32	2.36	2.41	2.352		
	$R_{1.GeSi}$[a]	Non-available[a]					
	2.45		2.32[a]	2.36[a]			
	$^{R}1.GeGe$		2.48	2.39	2.352		
Only Strained							
^{W}kj	SiSi		0.62	1.48	0.54		

^{C}kj	SiSi		0.62	0.52	0.54	0.53
R_1	$^{R}1.SiSi$	2.45	2.68	2.21	2.42	
	$^{R}1.SiG$		1.95	4.15	0.00	2.352

[a] Data not available in Refs. [10]; however $R_{1.GeSi} \equiv R_{1.SiGe}$ for configurations $^{2Ge2Si}T_{Si2}$ and $^{1Ge3Si}T_{Ge3}$, and for $^{1Ge3Si}T_{Si3}$ and $^{4Si}T_{Ge4}$.

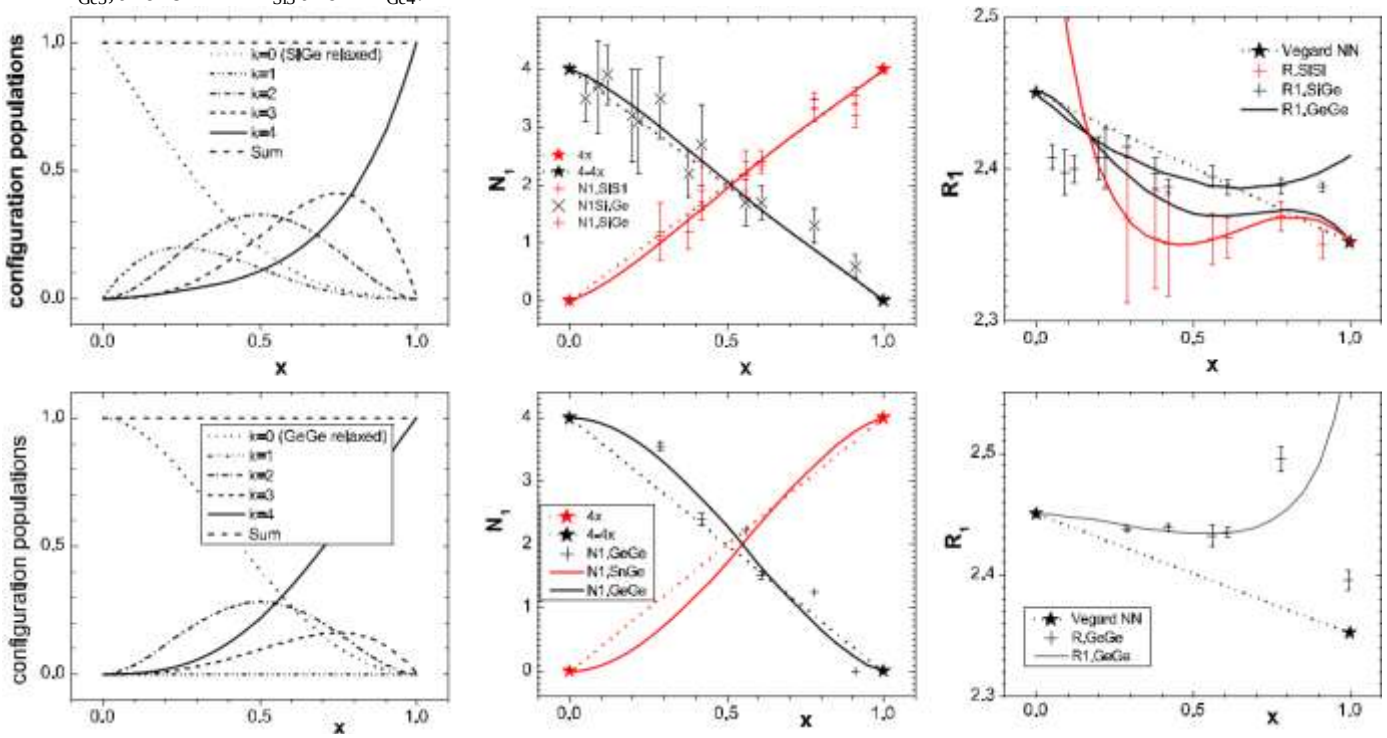

Fig. 1. $Ge_{1-x}Si_x$ from EXAFS data at the Si K-edge (top raw) and Ge Keedge (bottom raw) (left) Configuration populations, (center) N_1 and (right) R_1 values vs. x (relative to the full set of observed data listed in Table 1).

EXAFS bond-distance data from Ge- (R1.GeSi) or Si- (R1.SiGe) K-edge must give the same value to points R1.GeSi≡R1.SiGe. EXAFS-wise configurations (Table 2) 2Ge2SiTSi2 and 1Ge3SiTGe3 are equivalent, as are configurations $1Ge_3SiTSi_3$ and $4SiTGe_4$.

Table 3
$Ge_{1-x}Sn_x$ sample thicknesses [nm] and SRD's [%] from Ref. [32].

Sample	A2	A3	A4	A5	B1	B2	B3	B4	B5	C2	C3	C4	D1	D2	D3	D4	D5
x_{Sn} [%]	7.2	8.1	9.1	10.5	6.7	6.8	8.5	9.5	12	7.2	8.2	10.1	6	7.9	8.5	10.5	12.4
nm	68	45	59	45	144	113	112	118	116	210	240	213	542	499	420	305	466
SRD [%]	4	1	3	0	32	19	24	32	19	39	52	44	63	69	64	69	71

Table 4
$Ge_{1-x}Sn_x$ N_1, N_2 and R_1, R_2 values from Ref. [32].

	1	2	3	4	5	6	7	8	9	10	11	12	13	14	15	16	17
Sample	D1	B1	B2	A2	C2	D2	A3	C3	B3	D3	A4	B4	C4	A5	D4	B5	D5
^{x}Sn	0.06	0.067	0.068	0.072	0.072	0.079	0.081	0.082	0.085	0.085	0.091	0.095	0.101	0.105	0.105	0.12	0.124
$^{N}1.Ge$	3.4 (4)	3.8 (8)	3.7 (7)	4.0 (9)	3.5 (3)	3.7 (3)	3.6 (9)	3.8 (3)	3.3 (5)	3.3 (3)	4.0 (8)	3.0 (5)	3.1 (3)	3.9 (8)	3.4 (2)	3.4 (6)	3.1 (2)
$^{N}2.Sn$	1.3 (9)	1.6 (9)	2.5 (9)	1.8(X)	1.5 (9)	1.8 (6)	1.6(X)	1.5 (9)	1.2 (9)	1.8 (7)	1.4(X)	2.5 (9)	1.4 (7)	1.0 (5)	1.9 (7)	2.5 (9)	1.7 (6)

R_1	2.585 (9)	2.60 (1)	2.594 (9)	2.58 (2)	2.592 (4)	2.599 (5)	2.64 (3)	2.599 (5)	2.594 (9)	2.59 3	(42.61)(1)	2.604 (9)	2.587 (6)	2.6 (1)	2.595 (5)	2.59 (1)	2.599 (6)
R_2	4.00 (2)	4.10 (9)	4.05 (6)	4.00 (9)	4.01 (2)	4.08 (2)	4.08 (9)	4.04 (2)	4.04 (8)	4.01 (2)	4.11 (6)	4.02 (4)	4.03 (2)	4.01 (9)	4.05 (2)	3.98 (3)	4.07 (2)

Table 5
$Ge_{1-x}Sn_x$ W_{kj} and C_{kj} values of the tetrahedron configurations from available N_1, N_2 and R_1 (Table 4 in Ref. [32]).

k	0	1	2	3	4	$S(C_k)/3$
Configurations	$^{4Ge}T_S$ $_{n0}$	$^{3Ge1Sn}T_{Sn1}$	$^{2Ge2Sn}T_S$ $_{n2}$	$^{1Ge3Sn}T_{Sn3}$	$^{4Sn}T_S$ $_{n4}$	
^{W}kj	e	0.59	0	0		
^{C}kj	e	0.59	0	0	e	0.36
$^{R}1.Ge$	2.450	2.43	e	e	e	
$^{R}1.Sn$	e	3.46	e	e	2.810	
$^{R}2.GeGe$	4.007	4.31	e	e		
$^{R}2.SnSn$	e	3.93	e	e	4.589	

3. THE $GE_{1-X}SN_X$ ANALYSES.

Seventeen mono-crystalline $Ge_{1-x}Sn_x$ samples with fourteen x_{Sn}2[0.06, 0.124] concentrations were investigated by Gencarelli et al. at the Dutch-Belgian Beam-line DUBBLE (BM26A) of the European Synchrotron Radiation Facility (ESRF, Grenoble, France) at the Sn K-edge spectra. Synthesis and experimental procedures are available in Ref. [32]. Measurements on both strained and relaxed samples have been reported. Results are presented in four subsets: A, B, C and D each with at least three observations, which consents defining the three SOP-coefficients. Sample thicknesses and strain relaxation degrees (SRD) (Table 4) for $N_{1,Ge}$, $N_{2.Sn}$ and bond dis-tances (R_1) and (R_2) values at the Sn K-edge are listed in Table 5. Lacking the Ge K-edge spectra, only Sn-centered tetrahedra can be analyzed. As per Table 3, all samples A are thin in the range 2 [45e68] nm with a low SRD 2[0e4] %, samples B and C are medium thick 2[112 144] and 2[210 240] nm with SRD 2 [19e32] and 2[39e52] %, respectively and samples D are thick 2[305 542] nm with SRD 2[63e71] %.

Table 6
$Ge_{1-x}Sn_x$ W_{kj} and C_{kj} values of the tetrahedron-configurations best fitting the available N_1, N_2 and R_1 values for each A, B, C and D subset from Table 4.

k	0	1	2	3	4	$S(C_k)/3$
Configurations	$^{4Ge}T_S$ $_{n0}$	$^{3Ge1Sn}T_{Sn1}$	$^{2Ge2Sn}T_S$ $_{n2}$	$^{1Ge3Sn}T_{Sn3}$	$^{4Sn}T_S$ $_{n4}$	
A						
^{W}kj	e	0.68	0.39	0		
^{C}kj	e	0.68	0.39	0		0.36
B						
^{W}kj	e	0	0.89	0		
^{C}kj	e	0	0.89	0		0.30
C						
^{W}kj	e	0.78	0	0		
^{C}kj	e	0.78	0	0		0.26
D						
^{W}kj	e	0.44	0	0		
^{C}kj	e	0.44	0	0		0.15

From the values in Table 4 we derive the $[W_{kj}]_{k¼A,B;\ j¼1,3}$ and $[C_{kj}]_{k¼A,B;\ j¼1,3}$ values and the R_1 and R_2 values of the tetrahedron configurations (Table 5). Of the three configurations only $^{3Ge1Sn}T_{Ge1}$ is formed, with $C_{Sn,1}$ ¼ 0.59, $C_{Sn,2}$ ¼ 0, $C_{Sn,3}$ ¼ 0, with a mean value of 0.36. The analysis of distinct subsets indicates for A $C_{Sn,1}$ ¼ 0.59, $C_{Sn,2}$ ¼ 0, $C_{Sn,3}$ ¼ 0, with a mean value of 0.36, for B $C_{Sn,1}$ ¼ 0, $C_{Sn,2}$ ¼ 0.89, $C_{Sn,3}$ ¼ 0, with a mean value of 0.30, for C $C_{Sn,1}$ ¼ 0.78, $C_{Sn,2}$ ¼ 0, $C_{Sn,3}$ ¼ 0, with a mean value of 0.26, and for D $C_{Sn,1}$ ¼ 0.44, $C_{Sn,2}$ ¼ 0, $C_{Sn,3}$ ¼ 0, with a mean value of 0.15 (Table .6).

In all samples, the configuration $^{1Ge3Sn}T_{Sn3}$ is lacking. Apparently the increase of SRD enhances the structural stability. Moreover, the obtained set of SOPe$W_{Sn,j}$ values leads to a reasonable agreement among STM results and experimental values (Fig. 2).

4. CONCLUSIONS.

This manuscript describes the application of the Strained Tetrahedron Model to EXAFS spectra of binary alloys. We illustrated its application analyzing data of $Ge_{1-x}Si_x$ Ref. [10] and $Ge_{1-x}Sn_x$ Ref. [10] binary systems of the Group IV-IV of binary tetrahedron ordered B3 alloys. We determined the atomic distributions among the three strained tetrahedron-configurations although some conclusions are limited by the published data available.

The analysis of $Ge_{1-x}Si_x$ samples points out that from both Si and Ge K-edges, all three Si-centered tetrahedra are present, while in Ge-centered tetrahedra the $^{3Ge1Si}T_{Ge1}$ configuration is not detected and, at present, it is not clear the reason of the lack of this configuration. However, the expected behavior using the SOP-concept instead of the random Bernoulli distribution, matches reasonably well the discrete distribution emerging from the experimental data considering also the dispersion of some experimental points.

GeSn alloy spectra were collected only at the Sn K-edge, and we investigate the three Sn-centered tetrahedra. Of the three expected configurations only the $^{3Ge1Sn}T_{Sn1}$ configuration is detected. Within the present experimental limitations, the ST-model has been successfully applied on the available data of Group IV-IV binary tetrahedron ordered B3 alloys obtaining both the SOP coefficients W_{kj} and the corresponding attenuation factors C_{kj} of each random Bernoulli Eigen-function of the observed distorted tetrahedron configurations. This confirms once more the reliability of this model to investigate different binary alloys and its possible use for technological applications in materials science.

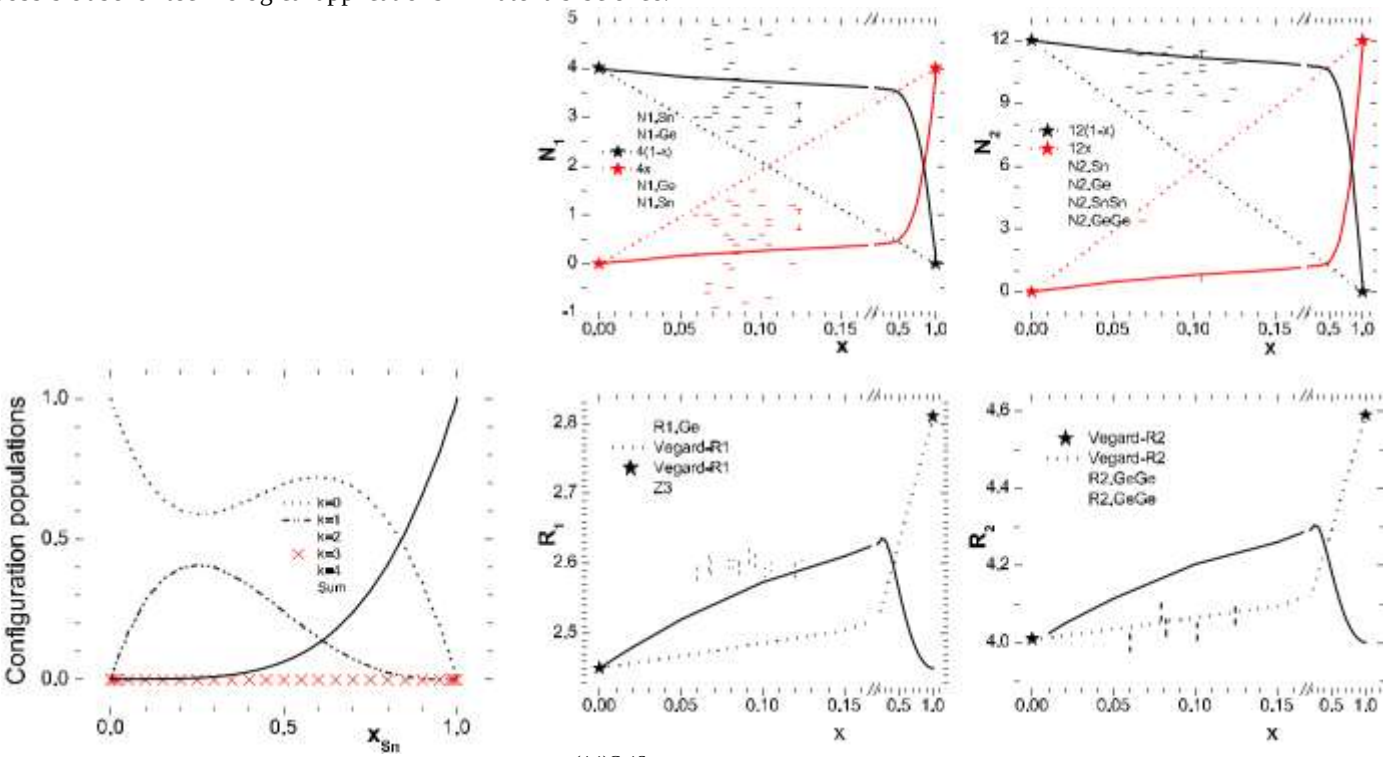

Fig. 2. Population distributions of the $Ge_{1-x}Sn_x$ of $[^{(4-j)GejSn}T_{k,j}]_{k¼Ge,Sn;j¼1,3}$ and of N_1, N_2, R_1, R_2 values (Vegard-lines) vs. x_{Sn} (experimental dataset listed in Table 4).

Acknowledgements

Authors acknowledge the financial support of the Russian Federation Assignment project _ N AAAA-A17-117022250040-0.

elements and those of binary Group IV-IV compounds that belong to the B3 crystalline group. The remaining six $[^{(4\ j)}{}_{BjA}T_{k,j}]_{k¼A,B;j¼1,3}$ have strained tetrahedron configurations to be determined.

Table
A1
Group IV elements and Group IV-IV binary: recovered lattice parameters a [Å], bond distances R_1 and dielectric constants: static ε_0 and dynamic ε_∞

Element	C	Si	Ge	Sn	Pb

a [Å]		3.567		5.431 [34]		5.658 [34]		6.489 [34]		6.852 [35]
R_1 [Å]		1.54 [34]		2.35 [34]		2.45 [34]		2.81 [34]		2.97
E_0		5.7000 [34]		11.6 [34]		16.00 [34]		23 [34]		
Binary	SiC	GeC	GeSi	SnC	SnSi	SnGe	PbC	PbSi	PbGe	PbSn
a [Å]	4.360 [35]	4.535 [35]	5.503 [35]	5.011 [35]	5.953 [35]	6.069 [35]	5.223 [35]	6.128 [35]	6.265 [35]	6.671 [35]
ε_0	9.72 [36]	12.08 [37]		34.57 [37]						
	10.28 [37]	8 [38]		10.27 [38]						
	7.1 [38,39]	7.2 [39]		13.6 [39]						
$\varepsilon\infty$	6.52 [36]	7.2 [37]	15.78 [40]	13.6 [37]	24.62 [40]	38.87 [40]				

REFERENCES

[1] N. Mousseau, M.F. Thorpe, Structural model for crystalline and amorphous Si-Ge alloys, Phys. Rev. B 48 (8) (1993) 5172.
[2] J.L. Martins, A. Zunger, Bond lengths around isovalent impurities and in semiconductor solid solutions, Phys. Rev. B 30 (10) (1984) 6217.
[3] M. Ichimura, et al., Calculation of bond lengths in $Si_{1-x}Ge_x$ alloys based on the valence-force-field model, Jpn. J. Appl. Phys. 29 (Part 1) (1990) 842.
[4] M.R. Weidmann, K.E. Newmann, Simulation of elastic-network relaxation: the $Si_{1\ x}Ge_x$ random alloy, Phys. Rev. B 45 (15) (1992) 8388e8396.
[5] S. de Gironcoli, P. Giannozzi, S. Baroni, Structure and thermodynamics of $Si_xGe_{1\ x}$ alloys from ab initio Monte Carlo simulations, Phys. Rev. Lett. 66 (16) (1991) 2116e2119.
[6] J.L. Martins, A. Zunger, Stability of ordered bulk and epitaxial semiconductor alloys, Phys. Rev. Lett. 56 (13) (1986) 6217e6220.
[7] J. Cai, et al., Electronic structure and B2 phase stability of Ti-based shape-memory alloys, Phys. Rev. B 60 (23) (1999) 15691e15698.
[8] Y. Cai, M.F. Thorpe, Length mismatch in random semiconductor alloys. I. General theory for quaternaries, Phys. Rev. B 46 (24) (1992) 15872e15878.
[9] N. Mousseau, M.F. Thorpe, Length mismatch in random semiconductor alloys. III. Crystalline and amorphous SiGe, Phys. Rev. B 46 (24) (1992), 15887-15887.
[10] J.C. Aubry, et al., First-shell bond lengths in $Si_{1ex}Ge_x$ crystalline alloys, Phys. Rev. B 59 (20) (1999) 12872e12883.
[11] B.V. Robouch, A. Kisiel, J. Konior, Statistical model for site occupation prefer-ences and shapes of elemental tetrahedra in the zinc-blende type semi-conductors GaInAs, GaAsP, ZnCdTe, J. Alloys Compd. 339 (1e2) (2002) 1e17.
[12] B.V. Robouch, et al., Occupation preference values in doped CmIm' multinaries from EXAFS and FTIR correlative analysis, Fiz. Nizk. Temp. 37 (3) (2011) 308e312.
[13] B.V. Robouch, et al., Strained-tetrahedra statistical model for atomic distances and site occupations in ternary intermetallic M3(X X^0) structures Ni_3(AlFe) case, J. Alloys Compd. 359 (1e2) (2003) 73e78.
[14] B.V. Robouch, et al., Statistical model analysis of local structure of quaternary sphalerite crystals, Low Temp. Phys. 33 (2) (2007) 214e225.
[15] B.V. Robouch, et al., Ion distribution preferences in ternary crystals $Zn_xCd_{1-x}Te$, $Zn_{1-x}Hg_xTe$ and $Cd_{1-x}Hg_xTe$, Eur. Phys. J. B 84 (2011) 183e195.
[16] B.V. Robouch, et al., Analysis of the phonon line profile of hydrogenated CdTe, J. Phys. Condens. Matter 20 (32) (2008) 325217e3252126.
[17] B.V. Robouch, et al., Statistical model structure of $A_{1-x}Z_xB_2$ Laves phase C15 system—the superconducting alloy $Ce_{1-x}La_xRu_2$, Low Temp. Phys. 35 (1) (2009) 116e121.
[18] B.V. Robouch, et al., First attempt to identify site occupation preference co-efficients of a quaternary alloy: the $InAs_xPySb_{1-x-y}$ system, J. Alloys Compd. 738 (2018) 218e223.
[19] B.V. Robouch, et al., GaAsPSb non random site occupation preference co-efficients of its multinary tetrahedron configurations, in: The Writing - Private Communication, vol. 13, 2017, 09.

[20] B.V. Robouch, A. Kisiel, EXAFS data resolved into individual site occupation preferences in quaternary compounds with tetrahedral coordinated structure,
J. Alloys Compd. 286 (1e2) (1999) 80e88.
[21] B.V. Robouch, et al., Far Infrared Spectra of Tetrahedral Quaternary Alloys Naukowyj Visnik Yzgorodskowo Univiersiteta, Seria Fizika, Vipusk, vol. 8, 2000, pp. 290e293, czastnica 2.
[22] B.V. Robouch, A. Kisiel, Ternary Elemental Zinc Blende Tetrahedra Size, Shapes, Preferences as Deduced from EXAFS Observations, in European Conf. On the Elementary Processes in Atomic Systems, Uzhgorod University Sci-entific Herald, Ukraine, 2000, pp. 67e73. Series Physics: Uzhhorod 25-28.07.
B.V. Robouch, A. Kisiel, J. Konior, Statistical model for atomic distances and site occupation in zinc-blende diluted magnetic semiconductors (DMSs), J. Alloys Compd. 340 (1e2) (2002) 13e26.
[23] B.V. Robouch, E.M. Sheregii, A. Kisiel, Statistical strained tetrahedron model of local ternary zinc blend crystal structures, Low Temp. Phys. 30 (11) (2004) 1225e1234.
[24] B.V. Robouch, et al., Statistical model of sphalerite structured quaternary $A1_xB_xY_yZ_{1-y}$ systems, J. Alloys Compd.s 426 (2006) 31e42, idem: Report LNF-06/04 (P) 9.02.2006 pp.1e20.
[25] B.V. R, A. Kisiel, A. Marcelli, Stoichiometry of Ternary Alloys beyond the Ca-nonical Bernoulli Distribution in IC SeNOB 2016, 2016 (Rzeszow, Poland).
[26] B.V. Robouch, A. Kisiel, Elemental Tetrahedra Sizes and Shapes of f.c.C. Zinc-blend Group III_V GaInAs and GaAsP, in 29th Intern. School on Physics of Semiconducting Compounds, 2000, p. 76. June 2-9 Ustron-Jaszowiec, Poland.
[27] B.V. Robouch, et al., Statistical Strained-Tetrahedra Model to Unfold Experi-mental Data of Ordered Intermetallic $M_3(X_{1-x}X'_x)_1$ and Zincblende Ternary Alloys for Preferences and Sizes of Elemental Terahedra, in 4th Moscow In-ternational ITEP School of Physics, 2001, pp. 113e126. Gordon & Breach February 5-16 Zvenigorod Moscow, Russia.
[28] B. Robouch, E. Sheregii, A. Kisiel, Statistical Strained-Tetrahedron Model of Local Ternary Zincblende Crystal Structures, in 32nd ITEPh Winter School and 7th International Moscow School of Physics, Institute of Theoretical & Experimental Physics (ITEF): 16-26/Feb, Otradnoe-Moscow, Russia, 2004, pp. 175e184. ; idem: LNFe04/23 (P) 26.10.2004 pp.1e15.
[29] B.V. Robouch, et al., Local structure analysis of $Ga_{1-x}Al_xN$ epitaxial layer, J. Appl. Phys. 104 (7) (2008) 7, 073508-4 ; idem: LNF-04/21 (IR) 15.10.2004 report.
[30] B.V. Robouch, et al., A statistical model for the local structure of $(A_{1-x}Z_x)1B_2$ laves phase C15 ternary crystals e the superconductor $(CeLa)Ru_2$ solid solu-tion. Abst: Poster in X08 - 21st International Conference on X-Ray and Inner-Shell Processes, 2008 (Paris).
[31] F. Gencarelli, et al., Extended X-ray absorption fine structure investigation of Sn local environment in strained and relaxed epitaxial $Ge_{1-x}Sn_x$ films, J. Appl. Phys. 117 (9) (2015).
[32] A. Kisiel, B.V. Robouch, A. Marcelli, The status of art of the analysis of complex multinary semiconductor alloys, Opto-Electron. Rev. 25 (2017) 242e250.
[33] Landolt-Bornstein,€ Group III/22 Semiconductors: Subvolume: a - Intrinsic Properties of Group IV Elements & III-V, II-VI & I-VII Compounds, in Landolt-
Bornstein:€ Numerical Data and Functional Relationships in Science and Technology - New Series, Springer-Verlag, Berlin, 1989, pp. 176e192, 776.
[34] N. Hammou, A. Zaoui, M. Ferhat, Revisiting stabilities of cubic zincblende IV-IV materials from density functional theory, Phys. Status Solidi 14 (11) (2017).
[35] F. Patrick, W.J. Choyke, Static dielectric constant of SiC, Phys. Rev. B 6 (1970).
[36] R. Pandey, et al., A theoretical study of stability, electronic, and optical properties of GeC and SnC, J. Appl. Phys. 88 (11) (2000) 6462e6466.
[37] S. Majidi, S.M.E. Elahi, Amirhosein, F. Kanjouri, First principle study of elec-tronic and optical properties of planar GeC, SnC and SiC Nanosheets, Protect. Met. Phys. Chem. Surface 53 (5) (2017) 773e779.
[38] R. Khenata, et al., Full potential linearized augmented plane wave calculations of structural and electronic properties of GeC, SnC and GeSn, Physica B 336 (3e4) (2003) 321e328.
[39] B.H. Elias, Structural, electronic, elastic, optical and thermodynamical prop-erties of zinc-blende SiGe, SiSn and GeSn from first principles, Adv. Phys. Theor. Appl. 25 (2013) 82e91.